Neutralization of LC- and RC-Effects with Left-Handed and NGD Circuits

Blaise Ravelo

IRSEEM (Institut de Recherche en Systèmes Electroniques Embarqués), EA 4353, ESIGELEC,
Avenue Galilée, 76801 Saint Etienne du Rouvray, France.
Tel.: +33 (0)2 32 91 59 71 / +33 (0)6 45 33 47 22
Fax: +33 (0)2 32 91 58 59
*corresponding author, E-mail: blaise.ravelo@yahoo.fr

Abstract

This paper focus is on the neutralization technique of the unwanted parasitic effects on radio frequencies (RF) and digital electronic circuits. Most of parasitic effects induced in these circuits can be modeled by RC- and LC-networks. For canceling these disturbing effects, we can proceed with operation as transfer function neutralization in the considered operating frequency bands. The neutralization presented in this paper is developed by using first, a left-handed (LH) and negative group delay (NGD) circuits inspired from metamaterials. The theoretical approach illustrating the RC- and LC-effects neutralization is described. Synthesis relations enabling to determine the elements of required LH and NGD circuit correctors in function of the perturbation parameters are established. Numerical and experimental demonstrators are presented to validate the technique proposed.

Keywords: *Negative group delay (NGD), RC-/LC-effects, neutralization technique, left-handed (LH) circuit, signal integrity (SI).*

1. Introduction

Long ago, Sommerfeld and Brioullin [1-6] investigated the problem of the light propagation in the region of the dispersive media having dispersive refractive index $n(\omega)$ at the angular frequency ω. They pointed out theoretically that in this region which appeared generally within an absorption line, the group velocity $v_g(\omega)$ can be superluminal, i.e., greater than the vacuum speed of light c and can even become negative:

$$v_g(\omega) = c/\{\Re e[n(\omega)] + \omega \cdot \Re e[\partial n(\omega)/\partial \omega]\}. \quad (1)$$

In this case, we realize negative group velocity (NGV) phenomena. These later were confirmed by Garrett and McCumber by calculating in details, the possibility to propagate superluminally a Gaussian pulse [7]. They underlined that Gaussian output pulses still suffer little distortion from its initial one. The first experimental verification of this NGV phenomenon was performed in 1982, by Chu and Wong by using laser pulses propagating a GaP:N sample as shown in [8]. To verify the existence and illustrate the significance of this extraordinary phenomenon, many theoretical and experimental demonstrations were performed [8-16]. This counterintuitive phenomenon was explained from the pulse reshaping because of constructive and destructive interferences in the frequency band of anomalous dispersion. In this region, it was shown several times, that the group refractive index $n_g(\omega)$ can become negative [12-18]. In this case, the group velocity, which is defined as:

$$v_g(\omega) = c/n_g(\omega), \quad (2)$$

and the group delay $\tau(\omega)$ whose both are related by:

$$\tau(\omega) = L/v_g(\omega), \quad (3)$$

By considering a medium with length L can be also negative. To study this counterintuitive phenomenon in electronic domain, it is more general to start with the group delay parameter $\tau(\omega)$ instead of the group velocity $v_g(\omega)$. Moreover, for any device modelled by a transfer function $T(j\omega)$, the group delay can be determined directly via the analytical definition:

$$\tau(\omega) = -\partial \angle T(j\omega)/\partial \omega. \quad (4)$$

Since the early 1990s, the possibility to generate negative group delay (NGD) phenomenon has been confirmed in electronic domain thanks to the topology of circuit proposed by Chiao and his co-workers [19-22]. The first NGD circuit composed of an operational amplifier in feedback with passive networks mainly composed of resistor(s), inductance(s) and capacitance(s) as described in [23-24]. With this topology, Kitano and his collaborators highlight the meaning of the NGD phenomenon by using a circuit showing the occurrence of output voltage pulse wave front before the input one penetrating in the circuit [23-24]. In this case, they demonstrated visually that a LED at the output can be switched on before that one connected at the input of the NGD circuit. However, such NGD circuit operates only up to some hundreds kHz [23-25]. It was stated that the NGD effect does not contradict the causality principle [19-

26]. In addition, the left-handed (LH) lumped passive circuit capable to generate NGD effect for microwave signals up to GHz has been introduced by the group of Mojahedi [15-16]. The topology of this circuit was established from the 1D metamaterials modelling of the array split ring resonators having simultaneously negative permittivity and negative permeability. This extraordinary physical concept was, first, proposed by Veselago in 1968 [27] and then, experimented in the early 2000s by Pendry and Smith [28-31]. Several experiments confirmed the physical existence of the superluminal and NGD phenomena with negative refractive index media [32-37]. In the presence of losses, the NGD generated by NGD passive media is accompanied by excessive losses [15-16, 38-40]. So, the applications are still limited in low frequencies. To overcome this physical roadblock, more recently, NGD active topologies for microwave signals were proposed [41-44]. These active topologies are constituted by RF transistor or amplifier associated with passive lumped networks. It was demonstrated theoretically and experimentally that these circuits are capable to generate simultaneously significant NGD level and amplification, and respecting all criteria of microwave active devices as the access matching and stability. The time delay limitation of NGD circuits is investigated in [45-46].

Based on the NGD function, different applications for the design of innovative oscillator [47], balun [48], phase shifters [49-51], pulse compression generator [52] and feed forward amplifier [53-54] were developed in electronic areas. In addition, further applications for the reduction of signal delays were also proposed based on the neutralization of the disturbing effects in the electronic systems [51][55-57]. The neutralization technique proposed in [57] is interesting for reducing the degradation caused the electrical interconnections in the printed circuit board (PCB) and microelectronic systems instead of the technique based on the use of repeaters [58].

With the increase of the operating data speed, the microelectronic signals propagating through the PCB interconnections and wireless propagation channels are victim of undesired degradations [59-64]. In circuit approach, this later can be usually modelled by RC-, LC- and RLC-networks. To reduce these effects, an efficient technique enabling to annihilate the RC-delay was also introduced by using base band NGD circuits [57]. It was shown that the RC-effect for high-speed applications can be cancelled [51]. Till now, few methods are available to neutralize the typically resonating effects modelled by LC-networks. For this reason, LC-effect neutralization techniques are developed in this paper by using LH- and NGD-circuits operating with modulated signals.

To highlight the feasibility of this concept, theoretic, simulation and experimental analyses are performed. Section 2 introduces the fundamental principle of the neutralization technique proposed. The next three sections are the applications of this technique for cancelling the undesired electrical effects modelled by base band and resonating networks. The final section is the general conclusion.

2. Fundamental principle of the neutralization technique proposed

The unintentional parasitic circuits occurred in the most of physical systems can be modelled by black box of the transfer function denoted T_d. Ideally, the neutralization technique can be traduced by the implementation of a system with outputs equal to its inputs ($v_{in} = v_{out}$). In this case, by denoting s the Laplace variable, the transfer function should be equal to unity as introduced in [51]:

$$T(s) = V_{out}(s)/V_{in}(s) = 1. \quad (5)$$

To achieve this operation, the parasitic function can be multiplied with the corrector transfer function mathematically defined as [51]:

$$T(s) = T_d(s) \cdot T_{corrector}(s) \approx 1 \Rightarrow T_{corrector}(s) = 1/T_d(s). \quad (6)$$

This analytical solution can be implemented by cascading the system T_d with $T_{corrector}$. So, one proposes to exploit the configuration presented by the block diagram depicted in Fig. 1.

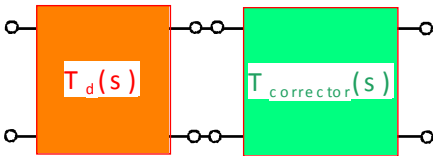

Figure 1: Disturbing system in cascade with the correction system [50]. In the ideal case, the frequency responses as the magnitude, phase and group delay of the correction system must be respectively expressed as:

$$T_{corrector}(\omega) = 1/T_d(\omega), \quad (7)$$

$$\varphi_{corrector}(\omega) = \angle T_{corrector}(j\omega) = -\angle T_d(j\omega), \quad (8)$$

$$\tau_{corrector}(\omega) = -\partial\varphi_{correction}(\omega)/\partial\omega = \partial\angle T_d(j\omega)/\partial\omega. \quad (9)$$

In the remainder of this paper, these expressions will be used for synthesizing neutralization circuits in function of the disturbances.

3. LC-effect cancellation with LH active circuits

Since the early 2000s, various microwave engineering applications of the LH concept have been proposed in the literature [65-68]. So, innovative microwave devices (filter, antenna, power divider, coupler…) were designed [65-68]. At the beginning, the LH-circuits were inspired thanks to the analogy with the metamaterials susceptible to operate with negative phase- and/or group-velocities [69-71]. Contrarily to the classical transmission lines which are categorized as right-handed (RH) structures, these LH circuits exhibit positive phase values in certain frequency bands.

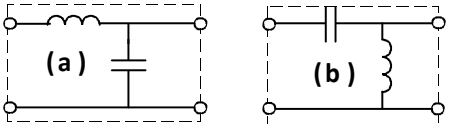

Figure 2: Purely (a) RH- and (b) LH- elementary cells.

One of the most expanded applications of these circuits is based on the use of composite right- and left- handed (CRLH) cells which are composed of LC- and CL-circuits

as shown in Fig. 2 [70-71]. However, the application of LH circuits is somehow restricted due to losses of input reflection and mismatch. Therefore, different numerical approaches dedicated to the analysis of LH structures were proposed [72-75]. In this section, a synthesis method of LH active cell for the neutralization of the LC-effect is introduced. To get more insight about the functioning of this LH active concept, a theoretical analysis on the cancellation technique of the LC-effect is presented based on the examination of the S-parameters. Then, validation results are presented and discussed.

3.1. Theoretical approach on the LC-effect neutralization technique

For compensating the LC-effect, we use LH active circuit based on the configuration explained in Fig. 3. It consists of cascading the disturbing LC-network with an active circuit formed by a transistor ended by LH cell.

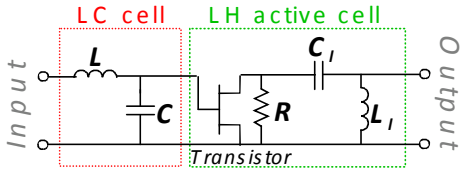

Figure 3: LC-circuit compensated with LH active circuit.

Along this study, to simplify the analytical expression, the transistor is supposed comprised of a transconductance g_m and a drain-source resistance R_{ds}, here, included in the matching resistance R. Therefore, the scattering parameters of the circuit shown in Fig. 3 are expressed as:

$$S_{11}(j\omega) = (LC\omega^2 - 1 + j\omega Z_0 C)/(LC\omega^2 - 1 - j\omega Z_0 C), \quad (10)$$

$$S_{12}(j\omega) = 0, \quad (11)$$

$$S_{21}(j\omega) = \frac{-2g_m R Z_0 L_l C_l \omega^2}{(LC\omega^2 - 1 + j\omega Z_0 C)\left[Z_0(L_l C_l \omega^2 - 1) - j\omega(L_l - RZ_0 C_l)\right]}, \quad (12)$$

$$S_{22}(j\omega) = \frac{[Z_0(1 - L_l C_l \omega^2) + RL_l C_l \omega^2 - j\omega(L_l - RZ_0 C_l)]}{[Z_0(L_l C_l \omega^2 - 1) + RL_l C_l \omega^2 - j\omega(L_l + RZ_0 C_l)]}. \quad (13)$$

For the reference impedance denoted Z_0 = 50Ω, by supposing:

$$C = 1/(L \cdot \omega_0^2), \quad (14)$$

with ω_0 is an angular frequency, the magnitude and phase of the transmission parameter S_{21} of the LC-circuit alone are respectively given by:

$$A_{LC}(\omega) = \frac{2Z_0 L\omega_0^2}{\sqrt{Z_0^2 L^2(\omega^2 - 2\omega_0^2)^2 + \omega^2(L^4\omega_0^4 + Z_0^4)}}, \quad (15)$$

$$\varphi_{LC}(\omega) = \arctan\left\{\omega(Z_0^2 + L^2\omega_0^2)/\left[Z_0 L(\omega^2 - 2\omega_0^2)\right]\right\}. \quad (16)$$

To neutralize this attenuation and phase shift at the given frequency ω_1, this relation must be verified:

$$S_{21}(j\omega_1) = 1 \Leftrightarrow \begin{cases} |S_{21}(j\omega_1)| = 1 \\ \varphi_{S_{21}}(\omega_1) = 0 \end{cases}. \quad (17)$$

By solving this equation system, the following synthesis relations are established:

$$L_l = Z_0\sqrt{R}/\left[\omega_0\sqrt{R + Z_0}\right], \quad (18)$$

and

$$C_l = 1/\left[\omega_0\sqrt{R(R + Z_0)}\right]. \quad (19)$$

According to the desired value of the total transmission gain $|S_{21}|$, the transistor characteristic g_m must be equal to:

$$g_m = \frac{S_{21}\sqrt{\left|Z_0^4 - Z_0^2 \cdot R^2 + 4\omega_0^2 \cdot L^2 \cdot R^2\right|}}{\omega_0 \cdot L|Z_0 - R|\sqrt{Z_0 \cdot R}}. \quad (20)$$

In this case, the minimal value of the output parameter $S_{22}(\omega_1) = 0$ is obtained if:

$$R = Z_0(\omega_1^2 - \omega_0^2)/(\omega_1^2 + \omega_0^2), \quad (21)$$

It is noteworthy that when $\omega_1 = \omega_0$, the expressions of the compensating LH-cell elements introduced in (18) and (19) are transformed as:

$$L_l = \sqrt{Z_0 \cdot R}/(2\omega_0) \quad (22)$$

and

$$C_l = 1/(L_l \cdot \omega_0^2). \quad (23)$$

In this case, the transistor parameters can be extracted from the desired value of the output parameter S_{22} with formulae:

$$g_m = S_{21}\sqrt{Z_0 + R}/(\omega_0 \cdot L\sqrt{R}), \quad (24)$$

with

$$R = 4Z_0 \cdot S_{22}^2/(1 - S_{22}^2). \quad (25)$$

One recalls that the matching resistance R_m can be determined from the equivalent resistance relation $1/R = 1/R_{ds} + 1/R_m$. Meanwhile, the matching resistance can be defined with the equation $R_m = R_{ds} \cdot R/(R_{ds} - R)$.

To verify the relevance of this LC-effect cancellation technique, simulations are conducted in the next subsection.

3.2. Validation with SPICE simulations

First, it should be emphasized that the simulation results presented in this paper were run with the electronic and microwave circuit simulator Advanced Design System (ADS) from Agilent™. Then, during the simulations, an arbitrary LC-network with parameters L = 2 nH and C = 2.2 pF was considered. At the given frequency f_1 = 1 GHz, the LH active circuit elements L_l = 15 nH, C_l = 7.8 pF and R = 62 Ω are synthesized. Then, after sensitivity studies with tolerances fixed to ±10%, one gets the simulation results displayed in Figs. 4. These graphs illustrate the neutralization of the transmission gain S_{21} and phase p_{21}.

One can see that with LH active circuit parameter variations of 10%, S_{21} and p_{21} relative variations only of about 1.5% are found. In addition, analysis of the transistor parameter influences was also performed by varying first, g_m and fixing R_{ds} = 100 Ω, and then, varying R_{ds} and fixing g_m = 20 mS. Therefore, the results shown in Figs. 5 were realized. These later explain that the gain compensations can be

carried out from certain values of the used transistor parameters.

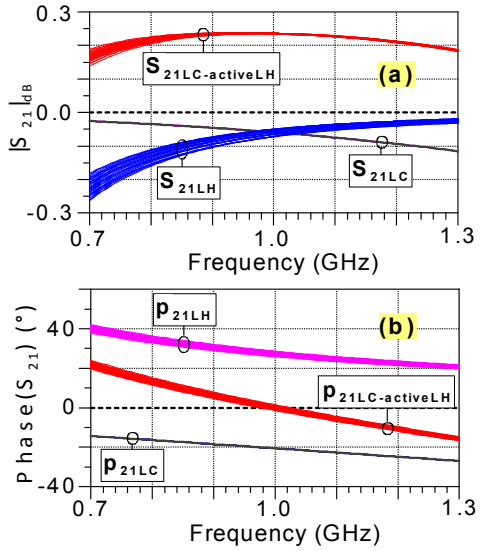

Figure 4: Magnitudes (a) and phases (b) of the LC, LH-cell and compensated circuit transmission parameters.

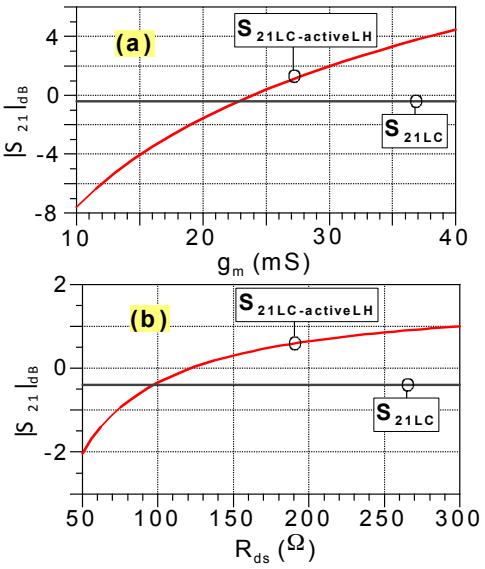

Figure 5: (a) $S_{21}(f_1)$ vs g_m and (b) $S_{21}(f_1)$ vs R_{ds}.

3.3. Remarks and discussions

A neutralization technique enabling to cancel out the LC-effect degradation is presented in this section by using an LH active circuit comprised of a transistor cascaded with a series capacitor ended by a parallel inductance. Synthesis expressions enabling to determine the compensator are established according to the operating frequency and the LC-parameters. To validate the synthesis method, results in very good agreement with the theory were found. In the continuation of this work, this technique will be used for improving the microwave device performances and the signal integrity (SI).

4. Resonating effects cancellation with NGD circuit for modulated microwave signals

The resonance phenomenon is one of the effects susceptible to disturb most of physical systems. In this section, we propose a cancellation technique of the resonance effect essentially modelled by parallel LC-network. To do this, the microwave NGD circuit formed by a transistor associated with RLC series network developed in [41-42] is used. Fig. 6 represents the configuration considered to perform this neutralization technique.

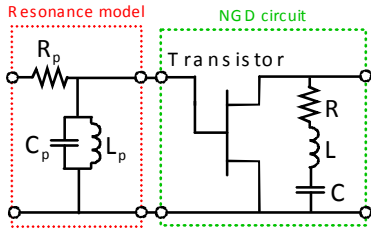

Figure 6: Resonating cell model in cascade with an NGD circuit.

Similar to the previous study established in section 3, the resonating circuit generating the perturbation is cascaded with the NGD circuit corrector.

4.1. Synthesis of the NGD circuits in function of the considered resonance parameters

The synthesis process introduced in this subsection is aimed to the determination of neutralizer elements in function of the perturbation $R_pL_pC_p$ around the resonance:

$$\omega_0 = 1/\sqrt{L_pC_p} = 1/\sqrt{L\cdot C}\,. \tag{26}$$

Around this frequency, one establishes that knowing the transistor characteristics, the S-parameters of the whole circuit shown in Fig. 6 are expressed as:

$$S_{21RLC-NGD}(\omega_0) = 2g_mZ_0R/(R+Z_0), \tag{27}$$

$$S_{22RLC-NGD}(\omega_0) = |R-Z_0|/(R+Z_0), \tag{28}$$

The corresponding group delay is equal to:

$$\tau_{RLC-NGD}(\omega_0) = \frac{2\left[\begin{array}{l}(R^2+Z_0R)(R_p+Z_0)\\ -Z_0L_pL\omega_0^2\end{array}\right]}{L_pR\omega_0^2(R+Z_0)}. \tag{29}$$

As aforementioned, the neutralization is realized when:

$$\begin{cases} S_{21RLC-NGD}(\omega_0) = 1 \\ \tau_{RLC-NGD}(\omega_0) = 0 \end{cases}. \tag{30}$$

By solving this last equation, we obtain the following synthesis formulae in function of the parameters R_p, L_p and C_p:

$$R = Z_0/(2Z_0\cdot g_m - 1), \tag{31}$$

$$L = R(R+Z_0)(R_p+Z_0)/(L_p\omega_0^2Z_0). \tag{32}$$

In this case, the capacitance value can be deduced by inverting equation (26).

4.2. Application results

To validate the concept, one proposes to neutralize the resonating effect with arbitrary parameters R_p = 43 Ω, L_p = 5 nH, C_p = 5 pF was performed. The resonance frequency is set at f_0 = 1 GHz. The employed transistor is characterized by the transcoductance g_m = 100 mS and the drain-source resistance R_{ds} = 200 Ω. By using relations (31) and (32), the following NGD circuit parameters R = 5.5 Ω, L = 2.9 nH and C = 8.7 pF are synthesized to perform the correction. The frequency responses of the whole circuit RLC-NGD under study are displayed in Fig. 7. As we can see, the $R_pL_pC_p$ circuit generates a significant attenuation more than -3 dB and positive group delay close to 400 ps around f_1. Thus, thanks to the gain and group delay behaviours of the NGD circuit, a total gain around 0 dB with very good flatness and a group delay near zero thanks to the NGD going down up to about -1 ns are realized. As expected, we find that the total transmission parameter responses (plotted in black lines) are close to unity.

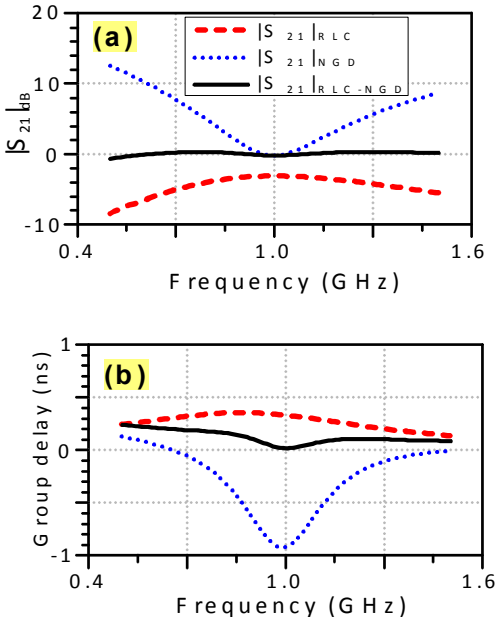

Figure 7: Transmission parameters of the circuit presented in Fig. 6. (a) Magnitude and (b) group delay.

5. RC-effect cancellation with base band NGD circuits for the analogue-digital signal

In this section, the neutralization technique under study is applied for enhancing the high-speed analogue-digital or mixed SI. To do this, after illustration on the used NGD circuit functioning developed in [51, 58-59], the analytical approach based on the transfer function of the RC-model and the RCNGD-circuit including the corrector NGD circuit will be explored. Then, validation experimental results will be explored.

5.1. Experimentation of the proposed base band NGD circuit

Fig. 8 depicts the base band NGD cell under study. The fabricated proof of concept is comprised of the PHEMT ATF-34143 transistor manufactured by Avago Technology™ supplied with V_{gs} = 0, V_{ds} = 3 V and I_{dss} = 110 mA. By using the ADS Momentum environment, the layout of the hybrid planar circuit was designed and implemented. It is noteworthy that this circuit is printed on the epoxy substrate FR4 with permittivity ε_r = 4.3 and thickness h = 800 µm [41].

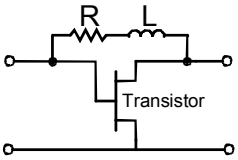

Figure 8: NGD circuit used (R = 56 Ω and L = 220 nH).

3.1.1. Frequency-domain results

To generate the magnitude and the group delay responses of the fabricated circuit, one proceeds with the traditional RF-circuit frequency measurement with vector network analyzer (VNA). Then, the transfer function was determined with the following relationship:

$$T(j\omega) = \frac{2S_{21}(j\omega)}{[1 + S_{11}(j\omega) - S_{22}(j\omega) - S_{11}(j\omega)S_{22}(j\omega) + S_{12}(j\omega)S_{21}(j\omega)]}. \quad (33)$$

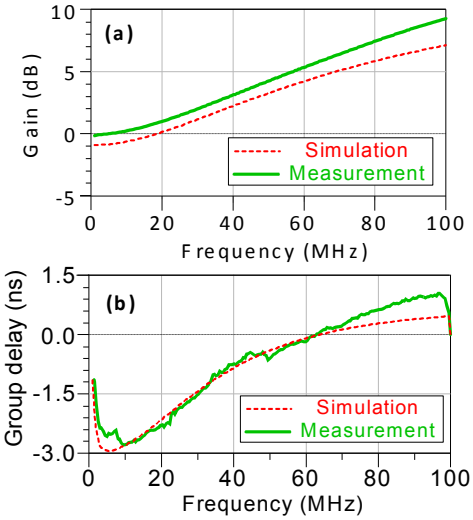

Figure 9: Comparisons of the simulated and measured frequency responses: (a) gain and (b) group delay [41].

As illustrated in Fig. 9(a), one obtains positive gain. The measured gain is slightly above the simulation, mainly due to the imperfection of the non linear model of the transistor used during the simulation. As revealed in Fig. 9(b), the measured group delay is well-correlated with the simulation. As expected, one observes that the prototype of the circuit tested provides a base band NGD up to 63 MHz which can go down below –2.5 ns.

3.1.2. Time-domain measurements:
The diagram presented in Fig. 10 illustrates the considered experimental setup. It consists to retrieve the input (CH1) and output (CH2) signals successively. The time domain measured result is displayed in Fig. 11. Thanks to the NGD effect illustrated in Fig. 9(b), output signal in time-advance of about 1.5 ns compared to the input one was observed.

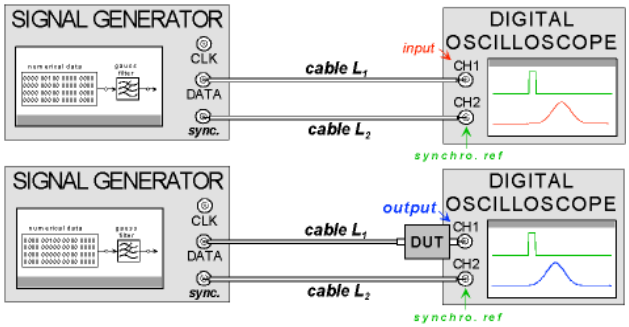

Figure 10: Diagram of the experimental setup [41].

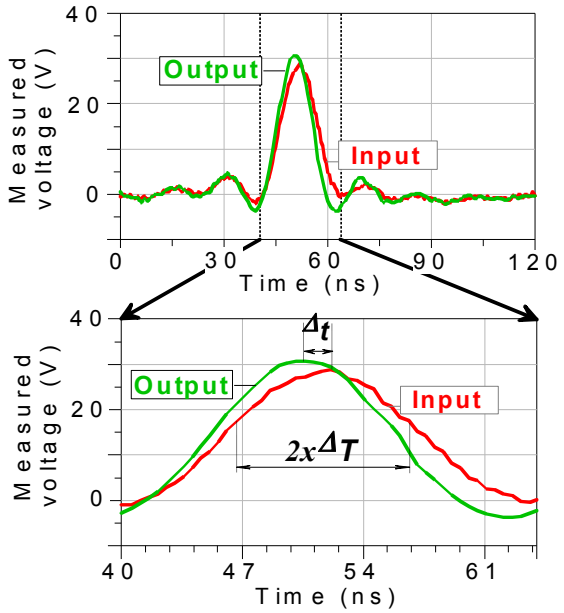

Figure 11: Time-domain measured input and output (opposite sign) pulses.

As sketched by the zoom in presented in the bottom of Fig. 11, the leading and trailing edges of the output are equally in time-advance of 1.5 ns. This result reveals the apparition of negative frontal velocity corresponding to the signal levels included in 10 % and 90 % of its maximal value. In fact, this extraordinary physical phenomenon can occur only when more than 95 % of the input power spectrum density belongs in the NGD frequency band. So that, smoothed input signal is necessary in order to realize this time-advance effect. However, the signals presenting discontinuity as unit step Heaviside cannot propagate in negative delay because its frequency spectrum is ideally infinite. One points out that the group velocity of the structure tested is v_g = -0.13c (c is the vacuum light speed).

In the next subsection, this NGD topology will be employed for neutralizing RC-effects.

5.2. Illustration of the neutralization effect in base band frequencies

As argued in section 2, in order to realize the neutralization effect, we use the NGD circuit in cascade with the parasitic model. According to relation (7), the corrector magnitude response T_{NGD} must behave as plotted in full line of Fig. 12(a) to cancel the attenuation induced by T_p [58]. Similarly for the group delay according to relation (9), we must generate the NGD τ_{NGD} as illustrated in Fig. 12(b) in base band frequencies to annihilate the delay τ_p.

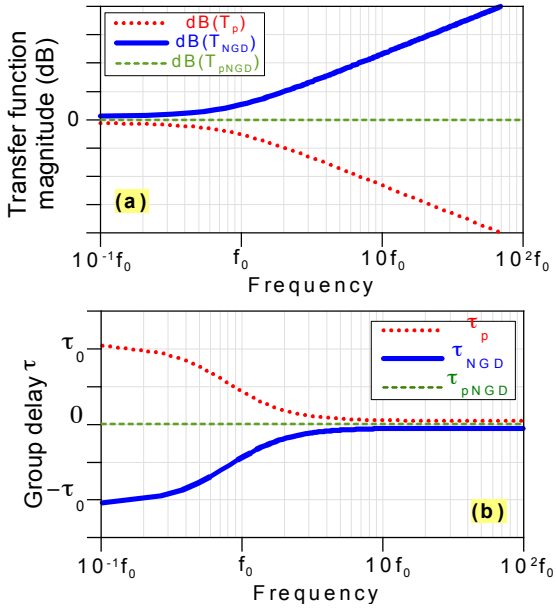

Figure 12: Illustration of the neutralization principle with frequency responses. (a) Magnitude and (b) group delay of the transfer functions $T_d(s)$ for the passive circuit, $T_{NGD}(s)$ for the NGD circuit and $T_{NGD}(s)$ for the cascaded system.

In the next subsection, these frequency responses will be experimented with the neutralization of the RC-effect with the NGD circuit presented in Fig. 6.

5.3. Analytical investigation of the RC-effect neutralization

Fig. 13 represents the diagram of the RC-circuit neutralized by the base band NGD circuit. One can establish that this circuit presents the transfer function and DC gain, respectively expressed as:

$$T(s) = \frac{R_{ds}(1-g_mR) - g_mR_{ds}Ls}{R + R_{ds} + R_c(1+g_mR_{ds}) + \left[R_cC(R+R_{ds}) + L\right]s + R_cCLs^2}, \quad (34)$$

$$T(0) = \frac{R_{ds}(1-g_mR)}{R + R_{ds} + R_c(1+g_mR_{ds})}. \quad (35)$$

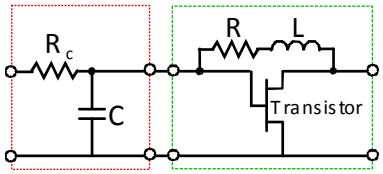

Figure 13: RC- and NGD active-circuit cascaded [51, 58].

Thanks to the neutralization technique, we are trying to reduce the 50% propagation delay induced by the RC-circuit alone which is analytically expressed as:

$$T_{rc} = R_c C\, ln(2). \quad (36)$$

To do this, in the next paragraphs, we will examine the frequency- and unit-step responses of the system defined by expression (34).

5.3.1. *Frequency responses of the RCNGD-system under study*

The transfer function expressed in (34) can be presented with the canonical form [58]:

$$T(j\omega) = \frac{\alpha_0 + j\omega\alpha_1}{\omega_n^2 - \omega^2 + 2j\zeta\omega_n\omega}. \quad (37)$$

where α_0 and α_1 are the real constants, and ω_n and ζ are respectively the undamped natural frequency and the damping ratio. Then, it yields the following magnitude and phase responses, respectively written as:

$$|T(j\omega)| = \frac{\sqrt{\alpha_0^2 + \alpha_1^2\omega^2}}{\sqrt{(\omega_n^2 - \omega^2)^2 + 4(\zeta\omega_n\omega)^2}}, \quad (38)$$

$$\varphi(\omega) = \arctan(\frac{\alpha_1}{\alpha_0}\omega) - \arctan(\frac{2\zeta\omega_n\omega}{\omega_n^2 - \omega^2}). \quad (39)$$

The corresponding group delay is given by:

$$\tau(\omega) = \frac{2\zeta\omega_n(\omega^2 + \omega_n^2)}{\omega^4 + 2(2\zeta^2 - 1)\omega_n^2\omega^2 + \omega_n^4} - \frac{\alpha_0\alpha_1}{\alpha_0^2 + \alpha_1^2\omega^2}. \quad (40)$$

As reported in [75], with $y(t)$ the unit step response of $T(s)$, the 50% Elmore propagation delay $T_{pd50\%}$ which is defined as:

$$y(T_{pd50\%}) = y(\infty)/2, \quad (41)$$

will be [64]:

$$\tau(0) = 2\zeta/\omega_n - \alpha_1/\alpha_0. \quad (42)$$

Knowing that compared to the exact value of the 50% propagation delay, (42) presents a relative error more than 30% due to the simplification of the exact model. For this reason, the study of the unit step response of $T(s)$ in the next paragraph.

5.3.2. *RCNGD-circuit unit step responses*

This response is obtained when the unit step signal presenting Laplace transform:

$$X(s) = 1/s \quad (43)$$

is injected at the input of the circuit shown in Fig. 16. The Laplace transform of the unit step response is given by:

$$Y(s) = T(s)X(s) = (\alpha_0 + \alpha_1 s)/(s^2 + 2\zeta\omega_n s + \omega_n^2)/s. \quad (44)$$

Similar to the classical second order passive system with constant numerator, according to the nature of $T(s)$ pole and the damping ratio ζ compared to 1, we classify three categories of unit step response $y(t)$ as shown by Fig. 14. We recall that according to the final value theorem:

$$y(\infty) = T(0) = \alpha_0/\omega_n^2. \quad (45)$$

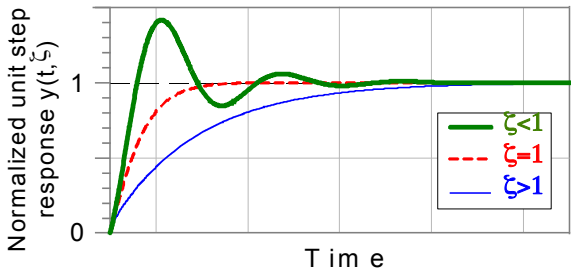

Figure 14: Three types of the unit step response of system (37) according to the damping factor ζ.

In the remainder of this paper, we denote y_{max} the maximum value of $y(t)$ at instant time t_{max}. So that, the overshoot is expressed as:

$$\xi = [1 - y(\infty)/y_{\max}] = [1 - T(0)/y_{\max}], \quad (46)$$

and the 50% propagation delay is the root of the equation:

$$y(T_{pd}) = \alpha_0/(2\omega_n^2). \quad (47)$$

5.3.3. *Case 1: $\zeta = 1$ Critically damping system analysis*

In this case, we have the unit step response:

$$y_1(t) = \{\alpha_0 - [\alpha_0 + (\alpha_0 - \alpha_1\omega_n)\omega_n t]e^{-\omega_n t}\}/\omega, \quad (48)$$

with the maximal value y_{1max} and overshoot ξ_1 at the instant time t_{1max} respectively given by:

$$y_{1\max} = \{\alpha_0 - (\alpha_0 - \alpha_1\omega_n)e^{-\alpha_1\omega_n/(\alpha_0 - \alpha_1\omega_n)}\}/\omega_n^2, \quad (49)$$

$$\xi_1 = (\alpha_1\omega_n/\alpha_0 - 1)e^{-\alpha_1\omega_n/(\alpha_0 - \alpha_1\omega_n)}, \quad (50)$$

$$t_{1\max} = \alpha_1/(\alpha_1\omega_n - \alpha_0). \quad (51)$$

It means that, the last one exists ($t_{1max} > 0$) when:

$$\alpha_1\omega_n - \alpha_0 \geq 0 \quad \Leftrightarrow \quad \alpha_1 > \alpha_0/\omega_n. \quad (52)$$

To keep the condition:

$$y_{1\max} \leq y_1(\infty) = \alpha_0/\omega_n^2, \quad (53)$$

we should expect the condition below:

$$\alpha_0 - \alpha_1\omega_n \geq 0. \quad (54)$$

Clearly, we see that this last condition is absolutely contrary to condition (52). According to expression (47), we propose another high accurate even exact solution below using the Lambert function $W(x)$ [77-78] defined as:

$$W(x)\exp[W(x)] = x. \quad (55)$$

Consequently, the 50% propagation delay will be:

$$T_{pd1} = [\alpha_0 + (\alpha_0 - \alpha_1\omega_n)W(x)]/[\omega_n(\alpha_1\omega_n - \alpha_0)]. \quad (56)$$

where:

$$x = (2\alpha_0 - \omega_n^2)e^{\alpha_0/(\alpha_1\omega_n - \alpha_0)}/[2(\alpha_1\omega_n - \alpha_0)]. \quad (57)$$

5.3.4. *Case 2: $\zeta > 1$ Over-damping system analysis*

In this case, the unit step response can be expressed as:

$$y_2(t) = y_{21}(t) + y_{22}(t), \quad (58)$$

where:

$$y_{21}(t)=\frac{\alpha_0}{\omega_n^2}+\frac{1}{2\omega_n^2}\left(\frac{\alpha_1\omega_n-\xi\alpha_0}{\sqrt{\xi^2-1}}-\alpha_0\right)e^{(\sqrt{\xi^2-1}-\xi)\omega_n t}, \quad (59)$$

$$y_{22}(t)=\frac{1}{2\omega_n^2}\left(\frac{\xi\alpha_0-\alpha_1\omega_n}{\sqrt{\xi^2-1}}-\alpha_0\right)e^{-(\sqrt{\xi^2-1}+\xi)\omega_n t}, \quad (60)$$

The optimal instant time is expressed as:

$$t_{2\max}=\frac{\ln\left(\frac{\xi\alpha_1\omega_n-\alpha_0+\alpha_1\omega_n\sqrt{\xi^2-1}}{\xi\alpha_1\omega_n-\alpha_0-\alpha_1\omega_n\sqrt{\xi^2-1}}\right)}{2\omega_n\sqrt{\xi^2-1}}. \quad (61)$$

This optimum exists under the condition:

$$\frac{\xi\alpha_1\omega_n-\alpha_0+\alpha_1\omega_n\sqrt{\xi^2-1}}{\xi\alpha_1\omega_n-\alpha_0-\alpha_1\omega_n\sqrt{\xi^2-1}}>0. \quad (62)$$

However, like the previous case, to avoid the overshoot or to keep:

$$y_{2\max}<y_2(\infty)=\alpha_0/\omega_n^2, \quad (63)$$

we must verify the opposite condition that is reduced to:

$$\alpha_1\omega_n(\xi-\sqrt{\xi^2-1})<\alpha_0<\alpha_1\omega_n(\xi+\sqrt{\xi^2-1}). \quad (64)$$

We can find that, $y_2(t)$ is dominated by $y_{21}(t)$ because $y_{22}(t)$ decreases rapidly when t increases. Since, the expanding second order Maclaurin series $y_{2a}(t)$ defined in (65) presents T_{pd} inaccurate than that involving from $y_{21}(t)$. So, we have T_{pd2} expressed in (66) yielded from the equation $y_{21}(T_{pd2})=\alpha_0/(2\omega_n^2)$.

$$y_{2a}(t)=\alpha_1 t+\left(\frac{\alpha_0}{2}-\xi\alpha_1\omega_n\right)t^2+O(t^3). \quad (65)$$

$$T_{pd2}\approx\frac{\ln\left[\frac{\alpha_0^2(\xi^2-1)}{(\alpha_0(\xi+\sqrt{\xi^2-1})-\alpha_1\omega_n)^2}\right]}{2\omega_n(\sqrt{\xi^2-1}-\xi)}. \quad (66)$$

5.3.5. *Case 3: $\xi<1$ Under damping system analysis*

In this last case, we have the unit step response $y_3(t)$ and the overshoot ξ_3 at t_{3max} respectively expressed as:

$$y_3(t)=\frac{\alpha_1\omega_n-\alpha_0\xi}{\omega_n^2\sqrt{1-\xi^2}}\sin(\omega_n t\sqrt{1-\xi^2})e^{-\xi\omega_n t}+\alpha_0/\omega_n^2\left[1-e^{-\xi\omega_n t}\cos(\omega_n t\sqrt{1-\xi^2})\right], \quad (67)$$

$$\xi_3=e^{-\xi\omega_n t_{3\max}}/\omega_n^2\sqrt{\alpha_0^2-2\xi\alpha_0\alpha_1\omega_n+\alpha_1^2\omega_n^2}, \quad (68)$$

$$t_{3\max}=\pi-\frac{\arctan\left[(\alpha_1\omega_n\sqrt{1-\xi^2})/(\alpha_0-\xi\alpha_1\omega_n)\right]}{\omega_n\sqrt{1-\xi^2}}, \quad (69)$$

Based on the time-domain behaviour of $y_3(t)$, we can assume that it presents an inflection point at T_i ($y_3''(T_i)=0$) which can be considered as its propagation delay and given by :

$$T_i=\frac{\arctan\left[\frac{(2\xi\alpha_1\omega_n-\alpha_0)\sqrt{1-\xi^2}}{\alpha_1\omega_n(2\xi^2-1)-\xi\alpha_0}\right]}{\omega_n\sqrt{1-\xi^2}}. \quad (70)$$

More accurate value of T_{pd} can be obtained by assuming $y_3(t)$ as its steepest slope of the thin black line displayed in Fig. 15. This line is defined from the tangent at the inflection point. Thereby, T_{pd3} will be the root of equation:

$$y_3'(t_i)(T_{pd3}-t_i)+y_3(t_i)=y_3(\infty)/2. \quad (71)$$

As result, the propagation delay can be written as:

$$T_{pd3}=t_i+[\alpha_0/(2\omega_n^2)-y_3(t_i)]/y_3'(t_i). \quad (72)$$

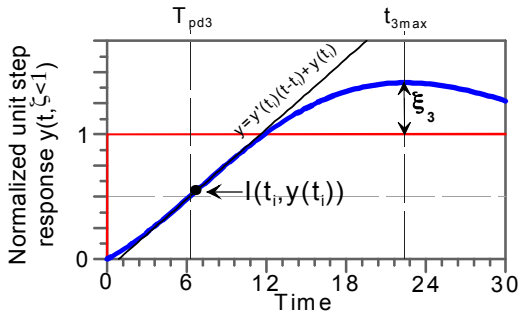

Figure 15: Unit step response of the second order active system for $\xi=0.3, \omega_n=4\pi 10^7, \alpha_0=2.25\omega_n^2$ and $\alpha_1=\omega_n$ illustrating the T_{pd3} approximation associated to the response to $\xi<1$.

5.4. Validation results

Fig. 16 displays the circuit diagram of the proof of concept. The PHEMT/ATF-34143 from Avago Technology™ was employed to implement the NGD circuit values compensating the RC-effect.

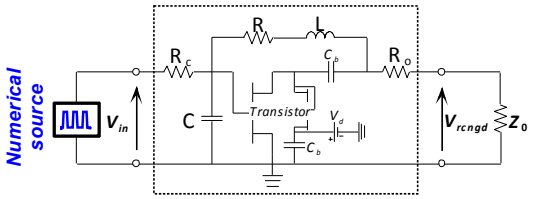

Figure 16: Schematics of the RCNGD-circuit including the biasing network using an FET = PHEMT ATF-34143 (V_{gs} = 0V, V_d = 3V, I_d = 110 mA), for R_c = 33 Ω, C = 680 pF, and R = 56 Ω, R_o = 10 Ω, L=220 nH, C_b=100 nF, Z_0 =50 Ω.

Figure 17: Photograph of the RCNGD-circuit implemented.

After application of the synthesis relations proposed in [57], the hybrid circuit comprised of surface-mount chip (SMC) passive components R, L and C displayed in Fig. 17 was manufactured. This prototype was printed on substrate-FR4 with permittivity $\varepsilon_r = 4.4$ and thickness $h = 800$ µm.

5.4.1. Measured frequency results of the neutralized circuit

The measured frequency results analysed in this paragraph were extracted from the S-parameters. Figs. 18 display the measured frequency responses of the RC-, NGD- and RCNGD-circuits from DC to 100 MHz. We can see that a very good correlation between the expected theoretic concept and the measurements is observed in Figs. 12.

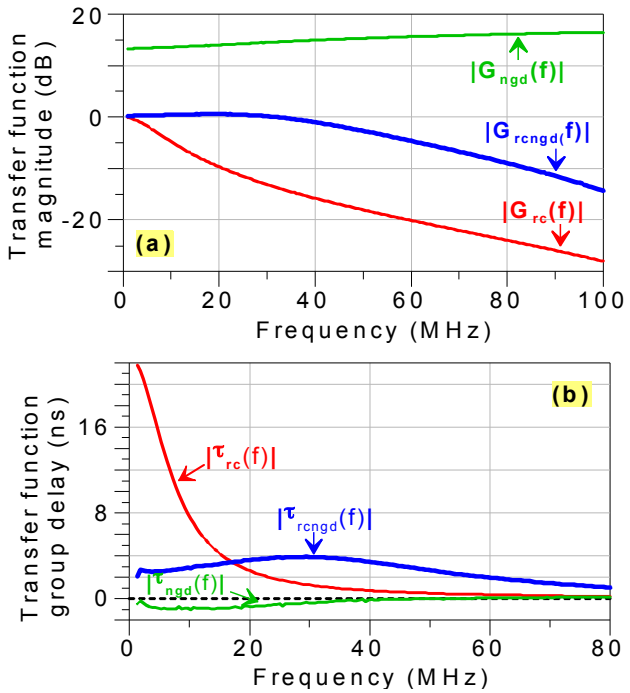

Figure 18: Measurement results of the transfer functions from the RC-, NGD- and RCNGD-circuits tested. (a) Magnitude and (b) group delay.

Once again, thanks to the gain level more than 10 dB up to 80 MHz and NGD of about -2 ns up to 55 MHz, a significant reduction of the RC-effects is observed. As consequence, the gain of the RCNGD-circuit is close to 0 dB up to 40 MHz whereas as shown in Fig. 18(b) the group delay is reduced strongly up to 20 MHz. These frequency responses illustrate the mechanism of the neutralization method proposed. To highlight more concretely the interpretation of this method, time-domain measurements were also performed. The next paragraph presents results obtained by considering analogue-digital input signals.

5.4.2. Time-domain experimental results

To confirm the proposed neutralization technique effectiveness for the SI improvement, we compare the square wave pulse v_{in}, and the RC- and RCNGD-circuit outputs, respectively denoted v_{rc} and $-v_{rcngd}$ as plotted in Fig. 19. So, we observe that compared to v_{rc}, the output $-v_{rcngd}$ is well-reconstructed and less distorted according to the input, v_{in}. As we can see in Fig. 19, the RC-circuit degrades the output leading edge with a rise time and a 50 % propagation delay respectively of $t_r \approx 35$ ns and $T_{rc} \approx 18.50$ ns. Due to the compensation with the NGD function, these parameters were respectively reduced to $t_{rngd} \approx 10$ ns and $T_{rcngd} \approx 2.50$ ns. It corresponds to the relative reduction: $(1 - T_{rcngd}/T_{rc}) \approx 71.4$ %, and $(1 - t_{rngd}/t_r) \approx 86.4$ %. In addition, an excellent improvement of the signal rising trailing edges is also achieved.

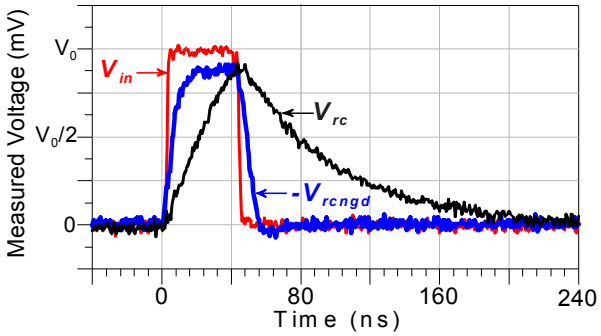

Figure 19: Time-domain measured results for the input square wave pulse with $V_0 = 1$ V with 25-Msym/s rate, 2 ns rise- and fall-times.

6. Conclusions

A neutralization technique enabling to suppress parasitic effects modelled by LC-, RC- and RLC-networks is developed in this paper. The basic principle of the neutralization concept is explained. The technique is based on the use of LH [71-72] and NGD active circuits inspired from the metamaterials. This reverse function circuits are susceptible to present transfer functions inverse of the parasitic networks under consideration.

To confirm the feasibility of the neutralization technique, various application examples of unwanted parasitic effects cancellation are developed theoretically, numerically and experimentally. First, the LC-effect neutralization is performed by using an LH active circuit. The synthesis relations in function of the LC-parameters are established. Then, simulations confirm the operability of the technique proposed at around 1 GHz. Then, a compensation of the resonance effect modelled by LC-parallel network by using an NGD circuit comprised of a transistor associated with an RLC-series network was also investigated. Numerical verifications confirm once again, the utility of the technique. The last use case application concerns the neutralization of the RC-effect with the base band NGD circuit proposed in [41]. The functioning of the NGD effect in base band frequencies was illustrated with experimentation of a circuit in hybrid planer technology. Output signal with front waves in time-advance of about 1.5 ns compared to the input ones is observed. Then, analytical investigation based on the frequency-response and unit step responses of the compensated RCNGD-circuit is presented. The relevance of the technique is confirmed with measured results both in the frequency- and in time-domains. By considering analogue-

digital signal with 25 Msym/s rate, a mixed SI improvement is demonstrated experimentally.

In the continuation of this work, the application of the neutralization techniques explored for enhancing RF-microwave/digital SI with mixed PCB is planned.

References

[1] Sommerfeld, "Ein Einwand gegen die Relativtheorie der Elektrodynamik und seine Beseitigung", *Physik. Z.* 8, pp. 841-842, 1907.

[2] Sommerfeld, "Uber die Fortpflanzung des Lichtes in Dispergierenden Medien", *Ann. Physik.* 44, pp. 177-201, 1914.

[3] L. Brillouin, *Wave Propagation in Periodic Structures*, McGraw-Hill, New York, 1946.

[4] Sommerfeld, *Vorlesungen über Theoretische Physik*, Band IV, Optik, Dieterich'sche Verlagsbuchhandlung, 1950.

[5] Sommerfeld, *Lectures on Theoretical Physics*, Optics. Academic Press Inc. US, 1954.

[6] L. Brillouin, *Wave propagation and group velocity*, Academic Press, New York, pp. 1-83 & 113-137, 1960.

[7] G. B. Garrett and D. E. McGumber, "Propagation of a Gaussian light pulse through an anomalous dispersion medium", *Phys. Rev. A*, Vol. 1, pp. 305-313, 1970.

[8] S. Chu. and S. Wong, "Linear Pulse Propagation in an Absorbing Medium", *Phys. Rev. Lett.*, Vol. 48, pp. 738-741, 1982.

[9] Ségard and B. Macke, "Observation of negative velocity pulse propagation", Phys. Lett. 109, pp. 213-216, 1985.

[10] Macke and B. Segard, "Propagation of light-pulses at a negative group-velocity", *Eur. Phys. J. D* 23, pp. 125-141, 2003.

[11] A. M. Steinberg and R. Y. Chiao, "Dispersionless, highly superluminal propagation in a medium with a gain doublet", *Phys. Rev. A*, Vol. 49, pp. 2071–2075, 1994.

[12] A. Dogariu, A. Kuzmich and L. J. Wang, "Transparent anomalous dispersion and superluminal light-pulse propagation at a negative group velocity", *Phys. Rev. A*, Vol. 63, pp. 053806.1-053806.12, 2001.

[13] L. J. Wang, A. Kuzmich and A. Dogariu, "Gain-assisted superluminal light propagation", *Nature 406*, pp. 277 – 279, 2000.

[14] K. T. McDonald, "Negative group velocity", *Amer. J. Phys.*, Vol. 69, No. 5, pp. 607–614, May 2001.

[15] O. F. Siddiqui, M. Mojahedi and G. V. Eleftheriades, "Periodically loaded transmission line with effective negative refractive index and negative Group velocity", *IEEE Transactions on Antennas and Propagation*, Vol. 51, No. 10, pp. 2619-2625, Oct. 2003.

[16] J. F. Woodley and M. Mojahedi, "Negative group velocity and group delay in left-handed media", *Phys. Rev. E*, Vol. 70, pp. 046603.1-046603.6, 2004.

[17] R. Y. Chiao, "Superluminal (but causal) propagation of wave packets in transparent media with inverted atomic populations", *Phys. Rev. A*, Vol. 48, pp. R34-R37, 1993.

[18] R. Y. Chiao, *Population inversion and superluminality, in amazing light*, Springer-Verlag, New York, pp. 91-108, 1996.

[19] R. Y. Chiao, E. L. Bolda, J. Bowie, J. Boyce and M. W. Mitchell, "Superluminality and amplifiers", *Prog. Crystal Growth Charact. Mat.* 33, pp. 319-325, 1996.

[20] M. W. Mitchell and R.Y. Chiao, "Causality and negative group delays in a simple bandpass amplifier", *Am. J. Phys.*, Vol. 66, pp. 14-19, 1998.

[21] M. W. Mitchell and R.Y. Chiao, "Negative group delay and 'Fronts' in a causal systems: An experiment with very low frequency bandpass amplifiers", *Phys. Lett. A*, Vol. 230, pp. 133-138, Jun. 1997.

[22] D. Solli, R. Y. Chiao and J. M. Hickmannn, "Superluminal effects and negative group delays in electronics, and their applications", *Phys. Rev. E*, Vol. 66, pp. 056601.1-056601.4, 2002.

[23] M. Kitano, T. Nakanishi and K. Sugiyama, "Negative group delay and superluminal propagation: An electronic circuit approach", *IEEE Journal of Selected Topics in Quantum Electronics*, Vol. 9, No. 1, pp. 43-51, Feb. 2003.

[24] T. Nakanishi, K. Sugiyama and M. Kitano, "Demonstration of negative group delays in a simple electronic circuit", *Am. J. Phys.*, Vol. 70, No. 11, pp. 1117-1121, 2002.

[25] J. N. Munday and R. H. Henderson, "Superluminal time advance of a complex audio signal", *Appl. Phys. Lett.*, Vol. 85, pp. 503-504, Jul. 2004.

[26] S. J. Erickson, M. Khaja and M. Mojahedi, "Time- and frequency-domain measurements for an active negative group delay circuit", *in Proc of IEEE Ant. Prop. Soc. Int. Symp.*, Vol. 3A, pp. 790-793, 2005.

[27] V. Veselago, "The electrodynamics of substances with simultaneously negative values of ε and μ", *Soviet Physics Uspekhi*, Vol. 10, No. 4, pp. 509-514, 1968.

[28] J. B. Pendry, "Negative refraction make a perfect lens", *Phys. Rev. Lett.*, Vol. 85, pp. 3966-3969, Oct. 2000.

[29] R. A. Shelby, D. R. Smith and S. Schultz, "Experimental verification of a negative index of refraction", *Science*, Vol. 292, No. 5514, pp. 77-79, Apr. 2001.

[30] J. B. Pendry, "Negative refraction", *Contemporary Physics*, Vol. 45, pp. 191-202, 3 May-June 2004.

[31] R. Smith, J. B. Pendry and M. C. K. Wiltshire, "Metamaterials and negative refractive index", *Science*, Vol. 305, pp. 788-792, 6 Aug. 2004.

[32] R. W. Ziolkowski and E. Hayman, "Wave propagation in media having negative permittivity and permeability", *Phys. Rev. E*, Vol. 64, pp. 056625.1-056625.15, 2001.

[33] R. W. Ziolkowski and A. D. Kipple, "Causality and double-negative metamaterials", *Phys. Rev. E*, Vol. 68, Part 2, pp. 026615, Aug. 2003.

[34] A. Dogariu, A. Kuzmich and L. J. Wang, "Transparent anomalous dispersion and superluminal light-pulse propagation at a negative group velocity," *Phys. Rev. A*, Vol. 63, pp. 053806.1-053806.12, 2001.

[35] R. W. Boyd and D. J. Gauthier, *'Slow' and 'Fast' light*, Ch. 6 in Progress in Optics 43, E. Wolf, Ed. Elsevier, Amsterdam, pp. 497-530, 2002.

[36] J. Gauthier and R. W. Boyd, "Fast light, slow light and optical precursors: What does it all mean", *Photonics Spectra*, pp. 82-90, Jan. 2007.

[37] A. Kuzmich, A. Dogariu, L. J. Wang, P. W. Milonni and R. Y. Chiao, "Signal velocity, causality and quantum noise in superluminal light pulse propagation", *Phys. Rev. Lett.* 86, pp. 3925-3929, 2001.

[38] S. Lucyszyn, I. D. Robertson and A. H. Aghvami, "Negative group delay synthesiser", *Electronic Letters*, Vol. 29, pp. 798-800, 1993.

[39] C. D. Broomfield and J. K. A. Everard, "Broadband negative group delay networks for compensation of oscillators using feedforward amplifiers", *Electronic Letters*, Vol. 20, pp. 1710-1711, Sep. 2000.

[40] N. S. Bukhman, and S. V. Bukhman, "On the negative delay time of a narrow-band signal as it passes through the resonant filter of absorption", *Radiophysics and Quantum Electronics*, Vol. 47, No. 1, pp. 66-76, 2004.

[41] B. Ravelo, "Demonstration of negative signal delay with short-duration transient pulse", *Eur. Phys. J. Appl. Phys.* (*EPJAP*), Vol. 55 (10103), pp. 1-8, 2011.

[42] B. Ravelo and S. De Blasi, "An FET-based microwave active circuit with dual-band negative group delay", *Journal of Microwaves*, *Optoelectronics and Electromagnetic Applications* (*JMOe*), Vol. 10, No. 2, pp. 355-366, Dec. 2011.

[43] B. Ravelo, "Investigation on microwave negative group delay circuit", *Electromagnetics*, Vol. 31, No. 8, pp. 537-549, Nov. 2011.

[44] B. Ravelo, "Baseband NGD circuit with RF amplifier", *Electronic Letters*, Vol. 47, No. 13, pp. 752-754, June 2011.

[45] M. Kandic and G. E. Bridges, "Asymptotic limits of negative group delay in active resonator-based distributed circuits", *IEEE Transactions on Circuits and Systems I: Regular Papers*, Vol. 58, No. 8, pp. 1727-1735, Aug. 2011.

[46] M. Kandic and G. E. Bridges, "Transient-imposed limitations of negative group delay circuits", *14th International Symposium on Antenna Technology and Applied Electromagnetics & the American Electromagnetics Conference (ANTEM-AMEREM), 2010,* Ottawa, ON, Canada, pp. 1-4, 5-8 July 2010.

[47] C. D. Broomfield and J. K. A. Everard, "Broadband negative group delay networks for compensation of oscillators using feedforward amplifiers", *Electronic Letters*, Vol. 20, pp. 1710-1711, Sep. 2000.

[48] B. Ravelo, A. Perennec and M. Le Roy, "Broadband balun using active negative group delay circuit", in *Proc. of the 37th European Microwave Conference*, Munich, Germany, pp. 466-469, Oct. 2007.

[49] S. Keser and M. Mojahedi, "Broadband negative group delay microstrip phase shifter design", *in Proc. of IEEE Ant. Prop. Soc. Int. Symp. 2009* (*APSURSI'09*), Charleston, SC, pp. 1-4, 1-5 June 2009.

[50] B. Ravelo, A. Perennec and M. Le Roy, "Synthesis of frequency-independent phase shifters using negative group delay active circuit", *Int. J. RF and Microwave Computer-Aided Engineering* (*RFMiCAE*), Vol. 21, No. 1, pp. 17-24, Jan. 2011.

[51] B. Ravelo, M. Le Roy and A. Pérennec, "Frequency-independent active phase shifters for UWB applications", *Proc. of the 40th European Microwave Conference*, Paris, France, pp. 1774-1777, 28-30 Sep. 2010.

[52] B. Ravelo, "Investigation on the microwave pulse signal compression with NGD active circuit", *PIER C Journal*, Vol. 20, pp. 155-171, 2011.

[53] H. Noto, K. Yamauchi, M. Nakayama, and Y. Isota, "Negative group delay circuit for feed-forward amplifier", *IEEE Int. Microw. Symp. Dig*., Honolulu, Hawaii, pp. 1103-1106, June 2007.

[54] H. Choi, Y. Jeong, C. D. Kim, and J. S. Kenney, "Bandwidth enhancement of an analog feedback amplifier by employing a negative group delay circuit", *PIER*, Vol. 105, pp. 253-272, 2010.

[55] K.-P. Ahn, R. Ishikawa, and K. Honjo, "Group delay equalized UWB InGaP/GaAs HBT MMIC amplifier using negative group delay circuits", *IEEE Transactions on Microwave Theory and Techniques*, Vol. 57, No. 9, pp. 2139- 2147, Sep. 2009.

[56] S. K. Podilchak, B. M. Frank, A. P. Freundorfer, and Y. M. M. Antar, "High speed metamaterial-inspired negative group delay circuits in CMOS for delay equalization", *in Proc. of 2nd Microsystems and Nanoelectronics Research Conference 2009 (MNRC 2009*), Ottawa, ON, Canada, pp. 9-12, 13-14 Oct. 2009.

[57] B. Ravelo and J. Ben Hadj Slama, "Equalization of digital/mixed-signal disturbances with an negative group delay circuit", *Proceedings of the 16th IEEE Mediterranean Electrotechnical Conference* (*MELECON 2012*), Yasmine Hammamet, Tunisia, 25-28 Mar. 2012, pp. 844-847.

[58] C.J. Akl, "Reducing Interconnect Delay Uncertainty via Hybrid Polarity Repeater Insertion", *IEEE Transactions on Very Large Scale Integration (VLSI) Systems*, Vol. 16, No. 9, pp. 1230-1239, Sept. 2008.

[59] S.-C. Wong, G.-Y. Lee and D.-J. Ma, "Modeling of interconnect capacitance, delay, and crosstalk in VLSI", *IEEE Transactions on Semiconductor Manufacturing*, Vol. 13, No. 1, pp. 108-111, Feb 2000.

[60] B. Ravelo, "Delay modeling of high-speed distributed interconnect for the signal integrity prediction", *Eur. Phys. J. Appl. Phys.* (*EPJAP*), Vol. 57, No. 3 (31002), pp. 1-8, Mar. 2012.

[61] T. Sakurai, "Closed-form expressions for interconnection delay, coupling, and crosstalk in VLSIs", *IEEE Transactions on Electronic Devices*, Vol. 40, No. 1, pp. 118-124, Jan. 1993.

[62] S. S. Sapatnekar, and I. A. Ames, "RC Interconnect Optimization under the Elmore Delay Model", *Proceedings of the 31st IEEE Conference on Design Automation*, 1994, San Diego, CA, 6-10 June 1994, pp. 387-391.

[63] S.-S. Myoung, B.-S. Kwon, Y.-H. Kim and J.-G. Yook, "Effect of group delay in RF BPF on impulse radio systems", *IEICE Transactions on Communications*, Vol. 90, No. 12, pp. 3514-3522, 2007.

[64] W. C. Elmore, "The transient response of damped linear networks", *J. Appl. Phys.*, Vol. 19, pp. 55-63, Jan. 1948.

[65] C.-Y. Liu, Q.-X. Chu and J.-Q. Huang, "A planar D-CRLH and its application to bandstop filter and leaky-wave antenna", *PIER Letters*, Vol. 19, pp. 93-102, 2010.

[66] O. Siddiqui, A. S. Mohra, and G. V. Eleftheriades, "Quad-band power divider based on left-handed transmission lines", *Electronic Letters*, Vol. 46, No. 21, pp. 1441-1442, Oct. 2010.

[67] C. Caloz, A. Sanada, and T. Itoh, "A novel composite right/left-handed coupled-line directional coupler with arbitrary coupling level and broad bandwidth", *IEEE Transactions on Microwave Theory and Techniques*, Vol. 52, pp. 980-992, Mar. 2004.

[68] R. Islam and G. V. Eleftheriades, "Phase-agile branch-line couplers using metamaterial lines", *IEEE Microwave Wireless Component Letters*, Jul. 2004, 14, Vol. 7, pp. 340-342.

[69] G. V. Eleftheriades, O. Siddiqui and A. K. Iyer, "Transmission line for negative refractive index media and associated implementations without excess resonators", *IEEE Microwave Wireless Component Letters*, Vol. 13, No. 2, pp. 51-53, Feb. 2003.

[70] A. Lai, C. Caloz and T. Itoh, "Composite right/left-handed transmission line metamaterials", *IEEE Microwave Magazine*, Vol. 5, pp. 34-50, Sep. 2004.

[71] T. Itoh, "Invited paper: Prospects for metamaterials", *Electronic Letters*, Vol. 40, No. 16, pp. 972-973, Aug. 2004.

[72] A. Levy, R. Shavit and L. Habib, "Optimisation of a microstrip left-handed transmission line using circuit modelling", *IET Microwaves, Antennas & Propagation*, Vol. 4, No. 12, pp. 2133-2143, 2010.

[73] S.-G. Mao, M.-S. Wu, Y.-Z. Chueh and C. C. Hsiung, "Modeling of symmetric composite right/left-handed coplanar waveguides with applications to compact bandpass filters", *IEEE Transactions on Microwave Theory and Techniques*, Vol. 53, No. 11, pp. 3460-3466, Nov. 2005.

[74] W.-R. Zhu, and X.-P. Zhao, "Numerical study of low-loss cross left-handed metamaterials at visible frequency", *Chinese Phys. Lett.*, 2009, 26 074212.

[75] Fu Jia-Hui, Wu Qun, Yang Guo-Hui, Meng Fan-Yi and Lee Jong-Chul, "Effective electromagnetic parameters of left-handed coplanar waveguide transmission lines", *J. Appl. Phys.*, Vol. 109, No. 7 (07A333), pp. 1-3, 2011.

[76] J. Vlach, J. A. Barby, A. Vannelli, T. Talkhan, and C. J. Shi, "Group delay as an estimate of delay in logic", *IEEE Transactions on Computed-Aided Design*, Vol. 10, No. 7, pp. 949-953, Jul. 1991.

[77] R. M. Corless, G. H. Gonnet, D. E. G. Hare, D. J. Jeffrey and D. E. Knuth, "On the Lambert W Function", *Advances in Computational Mathematics*, Vol. 5, pp. 329-359, 1996.

[78] D. J. Jeffrey, D. E. G. Hare and R. M. Corless, "Unwinding the branches of the Lambert W function", *Math. Scientist*, Vol. 21, pp. 1-7, 1996.